Moving Target Detection and Trajectory Estimation Using SAR Data

Paulo A.C. Marques
Instituto Superior de Engenharia de Lisboa / Instituto de Telecomunicações
ISEL-ADEETC – R. Conselheiro Emidio Navarro, 1, Lisboa
PORTUGAL

pmarques@isel.pt

ABSTRACT

Conventional Synthetic Aperture Radar processing leads to moving targets being imaged displaced from their real positions and blurred. This is mainly due to the used reference phase no longer being valid, including an additional Doppler-shift and a Doppler-spread. Since these effects are not considered in the focusing algorithm, the resulting SAR image shows the moving targets defocused and/or at wrong positions, depending on the motion direction. Basically, the Doppler-shift causes a misplacement of the moving targets in the azimuth direction, and the Doppler-spread causes their defocusing in the resulting image. This paper presents some state of the art algorithms that enable the focusing, repositioning, and trajectory estimation of the moving targets.

1.0 INTRODUCTION

Conventional Synthetic Aperture Radar (SAR) processing leads to moving targets being imaged displaced from their real positions and blurred [1]. This is mainly due to the used reference phase no longer being valid, including an additional Doppler-shift and a Doppler-spread. Since these effects are not considered in the focusing algorithm, the resulting SAR image shows the moving targets defocused and/or at wrong positions, depending on the motion direction. Basically, the Doppler-shift causes a misplacement of the moving targets in the azimuth direction, and the Doppler-spread causes their defocusing in the resulting image.

The development of multi-channel SAR systems facilitates implementation of sophisticated techniques for the detection and further processing of moving objects [2], [3].

It is well known that moving objects induce a variation on the Doppler history, that can be approximated as a quadratic function for low squint angles [4]; the variation of quadratic and linear terms causes, respectively, an azimuth smearing of the energy and an azimuth displacement of the peak, due to the mismatching of the reference function and the wrong range migration compensation.

The main difficulty is that the two velocity components are correlated, and the assumption of their independence is not correct, as will be shown in the next section.

The processing techniques for moving target processing can be divided into multi-channel and single-channel.

For the azimuth velocity estimation in multi-channel SAR systems, typical approaches consist in using Doppler rate filters to select the velocity that better focuses the target; for the range velocity estimation the techniques are based on the Doppler shift induced by the moving targets, as the Along Track Interferometry (ATI) [5]. Another popular type of estimation algorithm is called Space Time Adaptive Processing algorithms (STAP) [6] that requires an array of antennas.

Although multi-channel SAR systems are currently available, both airborne and space-borne, the raw data acquired by them is usually of restricted access. For the open scientific community only single channel data is typically made available, a context where moving target processing is more difficult.

This paper summarizes some state of the art algorithms published in recent literature that enable the focusing, repositioning, and trajectory estimation of moving targets using single channel SAR data. It starts by deducing the effects induced by a moving target on the SAR image algorithms. Then, it considers the modifications necessary to the wavefront reconstruction algorithm in order to correctly image the moving targets. A well-known limitation, the blind angle ambiguity, is addressed followed by the possibility of using the amplitude information, contained on the received echoes, to solve it. Section 3 presents a complete framework and summarizes several techniques recently published for moving targets processing using single channel SAR, such as digitally spotlighting the signatures, developing an ambiguity function for ground moving target indication (GMTI) and algorithms for their trajectory estimation. Section 4 draws the conclusions.

2.0 MOVING TARGETS PROCESSING

This section deduces the effects induced by moving objects on the received SAR signal, and present the modifications necessary to the wavefront reconstruction algorithm [7] in order to obtain focused. The blind angle ambiguity limitation is also addressed.

2.1 Focusing Moving Targets

Let us consider the scenario presented in Figure 1, where, for simplicity, a single moving target is present. The radar platform travels at speed v_R illuminating a moving point-like target with velocity $(v_x, v_y) = (\mu v_R, b v_R)$ defined in the slant-plane (x, y). Pair $(\mu, b) = (\frac{v_x}{v_R}, \frac{v_y}{v_R})$ is the target relative velocity with respect to the radar.

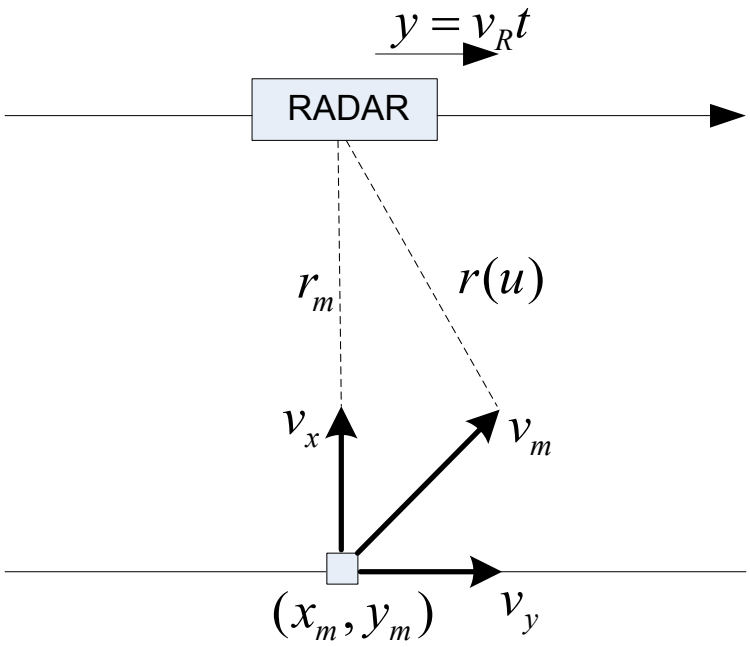

Figure 1: SAR Acquisition Geometry Considering a Single Moving Target.

When the radar is at position $u = 0$, the moving target coordinates are (x_0, y_0). The target distance from the radar, when the platform is at slow-time coordinate $y = u$, is:

$$r(u) = \sqrt{(x_0 - \mu u)^2 + [y_0 - (1+b)u]^2}. \tag{1}$$

Expanding the square-root arguments of (1) and denoting $v = 1 + b$, we get:

$$r(u) = \sqrt{X^2 + (Y - \alpha u)^2}, \tag{2}$$

where:

$$X^2 + Y^2 = x_0^2 + y_0^2, \tag{3}$$

$$\alpha Y = \mu x_0 + v y_0, \tag{4}$$

$$\alpha = \sqrt{\mu^2 + v^2}. \tag{5}$$

Following Soumekh's terminology (see [7] – Ch. 6.7), (X,Y) are the *motion-transformed coordinates*, $\sqrt{X^2 + Y^2}$ is the radial range, α_Y is the squint cross-range, and α is the relative speed.

Solving equations (3), (4), and (5) with respect to (x_0, y_0), we obtain:

$$\begin{bmatrix} x_0 \\ y_0 \end{bmatrix} = 1/\alpha \begin{bmatrix} v & -\mu \\ \mu & v \end{bmatrix} \begin{bmatrix} X \\ Y \end{bmatrix} \tag{6}$$

Therefore, the motion transformed coordinates (X, Y) are a rotation of angle $\text{atan}(\mu, v)$ of coordinates (x_0, y_0).

The fast-time Fourier transform of the received signal from a moving target can thus be written as:

$$s_m(\omega, u) = a(\omega, y_0 - vu) P(\omega) f_m e^{-j2k\sqrt{X^2 + (Y - \alpha u)^2}}. \tag{7}$$

To compute the slow-time Fourier transform of (7), the stationary phase method [1] is used. By noting that $a(\omega, u)$ is a smooth function of u when compared with the phase term:

$$e^{-j2k\sqrt{X^2 + (Y - \alpha u)^2}}, \tag{8}$$

we get:

$$S_m(\omega, k_u) = A(\omega, k_u) P(\omega) f_m e^{-j\sqrt{4k^2 - \left(\frac{k_u}{\alpha}\right)^2} X - j k_u / \alpha Y}. \tag{9}$$

If the parameter α is known, the wavefront algorithm can be applied to obtain focused images of moving targets. The only modification concerns the interpolation step which is now subject to:

$$k_X = \sqrt{4k^2 - \left(\frac{k_u}{\alpha}\right)^2}. \tag{10}$$

$$k_Y = k_u / \alpha \tag{11}$$

2.2 Blind Angle Ambiguity

The mapping from (x_0, y_0, μ, ν) to (X, Y, α) is not one-to-one; therefore, assuming that vector (X, Y, α) is known, we cannot determine unambiguously the complete moving target vector (x_0, y_0, μ, ν). In fact, we cannot determine the directions of vectors (μ, ν) and (x_0, y_0), but only their norm and the angle between them [1].

The undetermined nature of this problem is termed the blind angle ambiguity [9] or azimuth uncertainty problem.

Figure 2 illustrates the concept of blind angle ambiguity. It shows two moving targets with velocity vectors $v_i = (\mu_i, \nu_i)$, for i = 1, 2, and radar coordinates $x_i' = x_i - \mu_i u$ and $y_i' = y_i - \nu_i u$. Although the velocity vectors are different, their distances to the radar, $r = \sqrt{x'^2 + y'^2}$, are the same. Therefore, the phase term of the echoed signal from the moving targets does not have sufficient information, regarding the velocity vector direction.

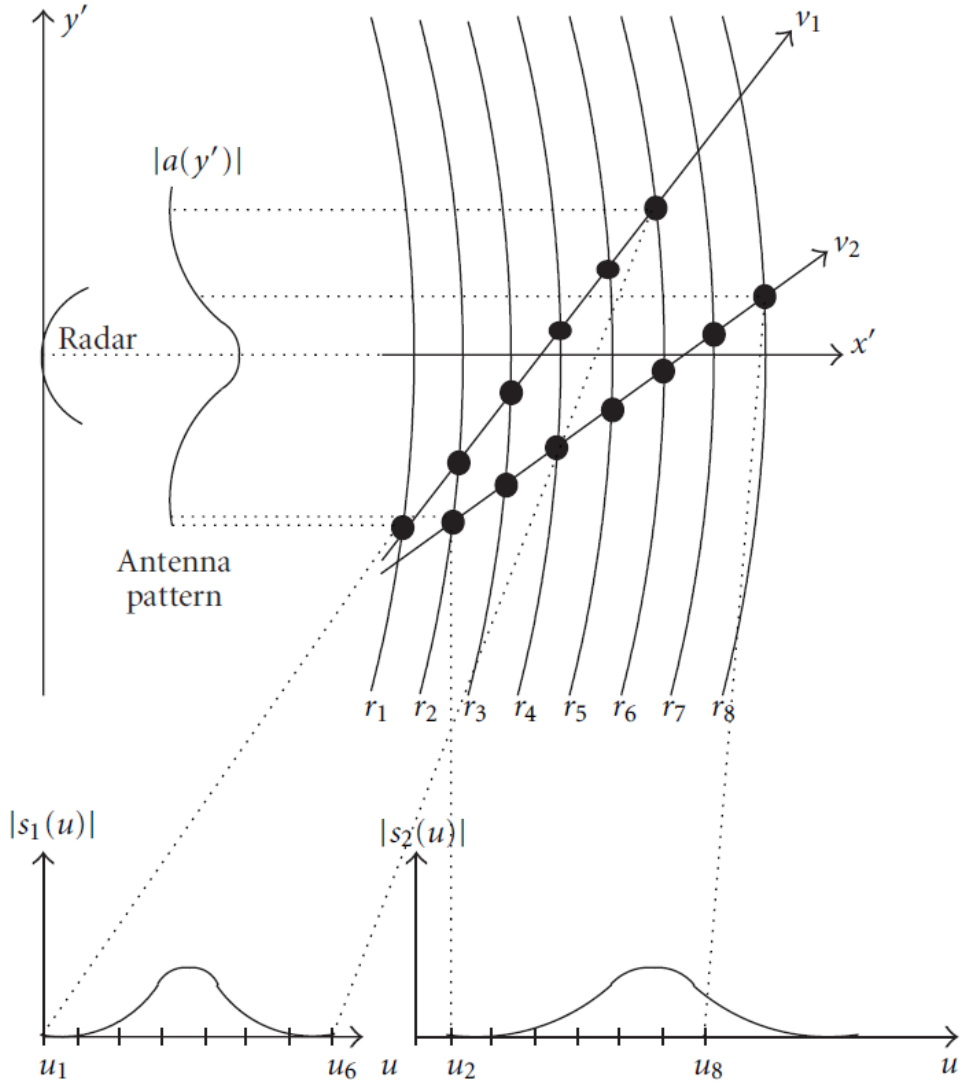

Figure 2: Two Moving Targets with Different Trajectories Can Induce the Same Phase on the Received Echoes $s_1(u)$ and $s_2(u)$.

Notice, however, that the echo amplitude $|s_i(u)|$ is a dilated and translated version of the antenna pattern. The dilation and translation are functions of the moving target parameters as illustrated in the plots of $|s_1(u)|$ and $|s_2(u)|$, at the bottom of Fig. 2. Some techniques that will be presented next exploit this fact to solve the blind angle ambiguity.

3.0 MOVING TARGETS PROCESSING

3.1 Digital Spotlight of Moving Target Signatures

In single channel SAR moving targets typically have to exhibit velocities such that they are outside the clutter spectrum in order to be detected. However some processing can be made to digitally increase the SCR of the scene.

The digital spotlighting operation is a digital signal processing process that isolates the signature of a moving target in a SAR scene and is presented in [7] – Ch. 6.7. This process can be simply described as a cropping of a scene in the region of interest. Therefore, most of the contribution of the global scene clutter is simply removed. This way, the ratio between power of signal echoed by the target and the (now residual) clutter is hugely increased.

A desired target signature may be digitally spotlighted in any of the domains such as, in the original slow-time and fast-time domains of the raw SAR data, or any other of its transformations, including the reconstruction domain. The reconstruction domain is often one of the more beneficial since the target signature has smaller dimensions, although the signal is defocused due to the motion effects, therefore permitting cropping of the smallest regions, with the corresponding clutter contribution reduction.

To perform moving target detection, the preferred domain to isolate the SAR signature of a specific target is the reconstruction domain, that is, the (x, y) domain of the coherent reconstructed image $f(x, y)$. In this domain the moving target signature is fairly focused and can be separated from the signatures of the other targets. Once the target signature is spotlighted in the (x, y) domain, it can be transformed to any domain of the SAR signal for further processing.

The summary of the signal processing involved is as follows. Consider the reconstructed target scene for the relative speed of $\alpha = 1$ (stationary situation). In this scenario, and if the *n*th target moves with a speed much smaller than the SAR platform, the moving target image, although defocused, will be fairly localized at the motion transformed coordinates:

$$(X_{nc}, Y_{nc}) \approx \left(X_n, \frac{Y_n}{\alpha_n}\right). \tag{12}$$

Denoting as R_n the region where the smeared signature of the *n*th target appears, its signature can be fairly reconstructed back to the (ω, u) domain, i.e. digitally spotlighted, by computing:

$$s_n(\omega, u) \approx \sum_{(X,Y)\in R_n} f(X_i, Y_j)\, exp\left[-j2k\sqrt{{X_i}^2 + (Y_j - u)^2}\right], \tag{13}$$

where $(X, Y) \in R_n$ are the complex pixel values of the cropped region R_n.

In fact, the signature of the moving target can be reconstructed back to any of the domains. Figure 3 illustrates the digitally spotlight operation on a SAR image containing a BTR-60. The target signature is then resynthesized to the (k, k_u) domain.

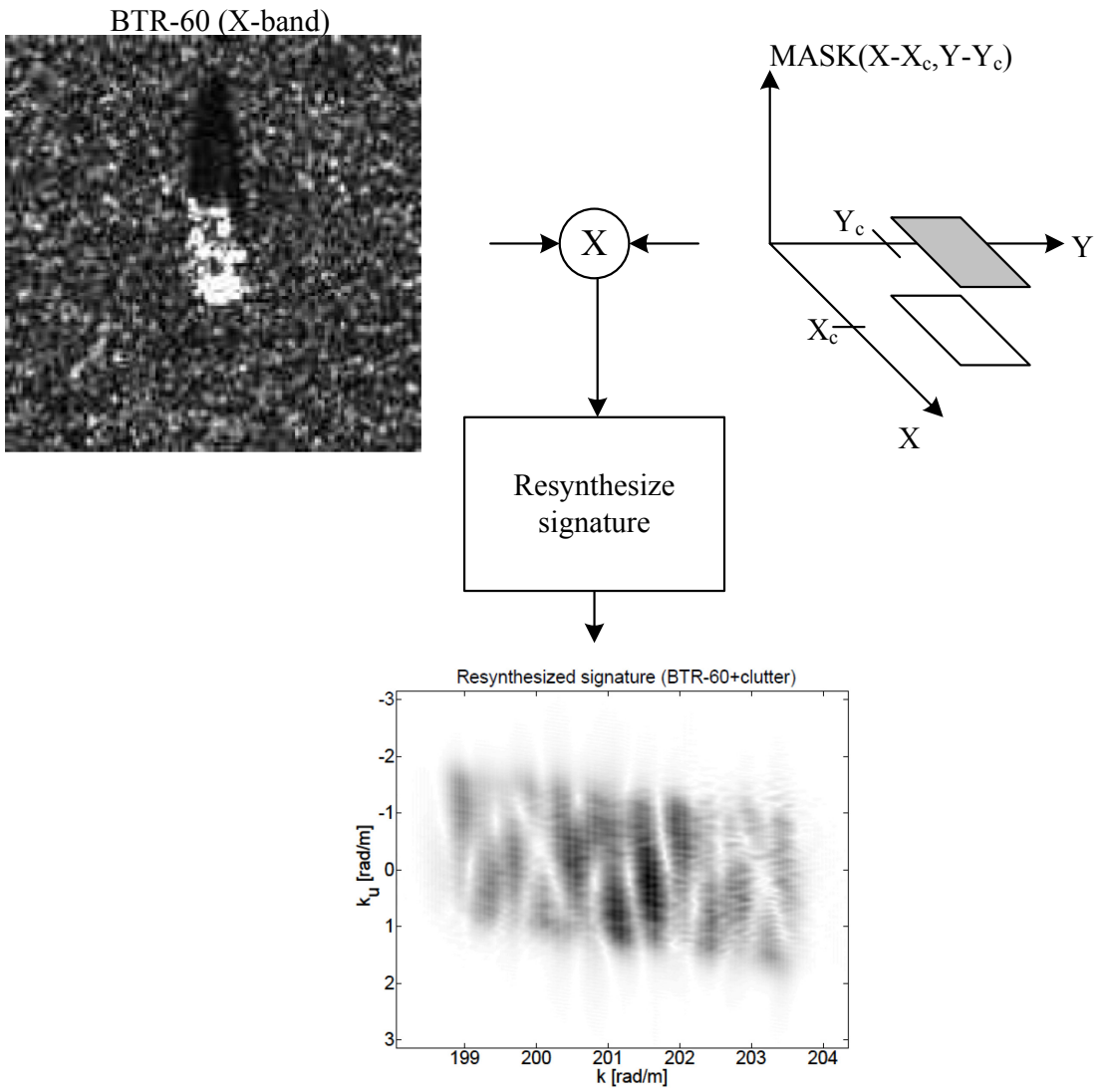

Figure 3: Digitally Spotlight of a Focused SAR Region Containing a BTR-60 from MSTAR Data. The signature is resynthesized to the (k, k_u) domain.

In summary, this technique can be applied to increase, synthetically, the SCR of the scene containing moving targets. Therefore, it permits the successful application of GMTI techniques for endoclutter moving targets using single channel SAR.

3.2 SAR Ambiguity Function for Ground Moving Target Indication

Soumekh proposes in [7] – Ch. 6.7 a SAR ambiguity function which simultaneously detects moving targets and estimates their relative velocity α.

The strategy starts by focusing the target area using the wavefront reconstruction algorithm with static ground parameters. Although the moving targets appear defocused and smeared, they will, hopefully, occupy a fairly localized region when compared with the target area dimensions.

The author then proposes to divide the target area into small overlapping subpatches, to resynthesize their SAR signature, and to apply the so-called SAR ambiguity function to the resynthesized signature. This SAR

ambiguity function consists in applying a phase compensation on the resynthesized signal, for all α's of interest, and then computing the Fourier transform in the slow-time dimension for a fixed ω. If a moving object is present in the subpatch, then the function exhibits a maximum for the correct α. Using the estimated α, the moving object can be correctly focused.

This technique has some weaknesses: To reduce the contribution from the clutter, the subpatches have to be small. However, small subpatches lead to a large number of regions to process, besides introducing a limit in the supported target smearing (which has to be smaller than the subpatch size), and, therefore, in the target maximum velocity.

The algorithm starts by performing the slow-time compression on the reconstructed signature $s_n(\omega, u)$ for the digitally spotlighted region R_n at the desired α corresponding to speeds of interest:

$$\eta_n(\omega, u, \alpha) = s_n(\omega, u) exp\left[j2k\sqrt{{X_{nc}}^2 + (Y_{nc} - \alpha)^2}\right] \tag{14}$$

The reference spatial point for the slow-time compression is the center of the region R_n, denoted here by (X_{nc}, Y_{nc}).

The SAR ambiguity function is computed by:

$$\mathrm{H}_n(\omega, u, \alpha) = FT_{(u)}[\eta_n(\omega, u, \alpha)], \tag{15}$$

for a fixed ω, typically corresponding to the central frequency f_c. Equation (15) will exhibit a peak for the value of α corresponding to the velocity of the moving target, if one is present. Otherwise, the peak will occur for $\alpha = 1$.

Figure 4 illustrates a typical SAR ambiguity function for a moving target. In this situation the peak occurs at $\alpha = 0.88$.

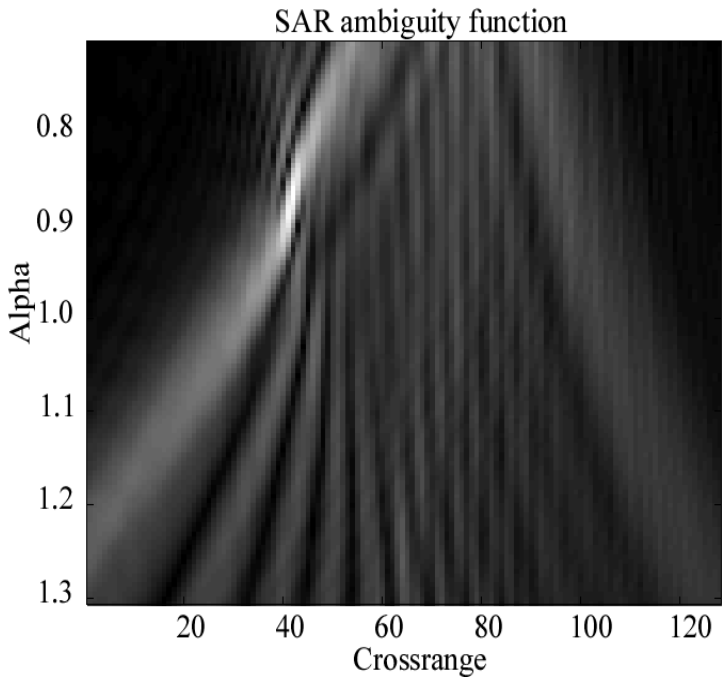

Figure 4: SAR Ambiguity for an Individual Moving Target with Relative Velocity $\alpha = 0.88$.

This technique is useful for scenes with SCR greater than 10 dB in the spotlighted region. Additionally it has the ability to detect endoclutter targets provided that there is a previous digital spotlight of the region under analysis. However it is unable to solve the blind angle ambiguity, i.e. estimate the direction of the moving target.

3.3 Directional Moving Target Indication

In [9] a modified version of the previously presented SAR ambiguity function, designated by Directional Moving Target Indication - DMTI, is proposed. The main novelty consists in introducing the capability to discriminate targets moving in a predefined direction of interest, reducing the contribution of traffic moving in undesired directions. The application of this methodology is, mainly, civil traffic monitoring using single channel SAR data. This discrimination ability may be a very important goal in traffic monitoring since the roads of interest (with known angles) have, typically, many roads nearby with different directions. These nearby roads may carry traffic which, otherwise, will be detected and may corrupt the estimation of the traffic parameters for the roads of interest.

The considered scenario is presented in Figure 5, where the moving target velocity magnitude is v_m and its direction is θ; the relative slant-range velocity is:

$$\mu(v_m, \theta) = \frac{v_m}{V} \cos\theta, \tag{16}$$

and the quantity related to the cross-range velocity is:

$$\nu(v_m, \theta) = 1 + \frac{v_m}{V} \sin\theta. \tag{17}$$

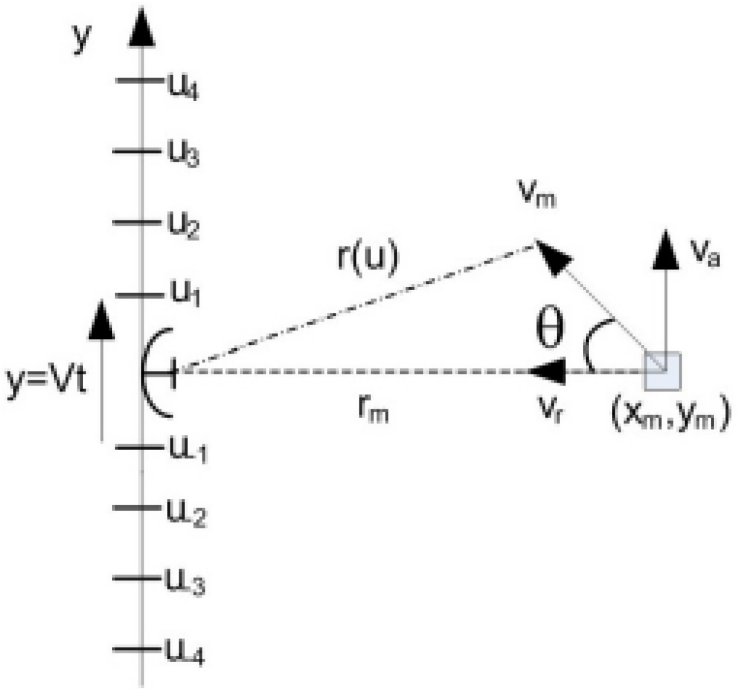

Figure 5: SAR Acquisition Geometry – DMTI.

Parameter α is thus computed by:

$$\alpha(v_m, \theta) = \sqrt{1 + \frac{v_m}{V}\left(\frac{v_m}{V} + 2\sin\theta\right)}. \tag{18}$$

The Doppler spread can therefore be compensated as function of (v_m, θ) and the unwanted targets can be filtered out, besides the static ground echoes, by using the antenna pattern function, as follows:

$$s_c(\omega, u, v', \theta') = s_m(\omega, u)\exp[j2k\psi(u, v', \theta')] * a^*(\omega, u, v', \theta'). \tag{19}$$

where:

$$\psi(u, v', \theta') = \sqrt{X_c{}^2 + [Y_c - \alpha(v', \theta')u]^2}. \tag{20}$$

The central coordinates of the region under analysis are denoted by X_c and Y_c. Parameters μ, ν, and α are computed by (3), (4) and (5).

For a moving target with parameters $(v_m, \theta_m) \approx (v', \theta')$, the Fourier transform of (19), with respect to slow-time u, will exhibit peaks, since the energy spread is compensated and the signal will not be filtered out by the term due to the antenna pattern. Therefore, the detection and estimation of moving targets with direction θ can be accomplished, in the slow-time frequency domain, by searching the absolute maxima of:

$$\begin{aligned}\varepsilon(\omega, k_u, v', \theta') \quad = \quad & A[\omega, k_u, \mu(v', \theta'), \nu(v', \theta')] \\ & \times FT_{(u)}\left[s_m(\omega, u)e^{j2k\sqrt{X_m^2 + [Y_m - \alpha(v', \theta')u]^2}}\right]\end{aligned} \tag{21}$$

for a fixed ω and a range of velocities v' of interest.

In real scenarios due to the low SCR and to the possible presence of several strong static scatterers, the SAR ambiguity function for the moving targets of interest may be completely dominated by the clutter ambiguity signature. Moreover, the targets signature in the Fourier domain may partially, or fully, overlap with that from the clutter, depending on the direction of interest. Therefore this technique, similarly to the one presented in the previous section, benefits of a previous enhancing of SCR by using the digital spotlight technique.

This technique reduces the contribution from most of the clutter and moving targets sufficiently apart from the region under study.

Range resolution is a measure of the resolvability of the targets in the range domain and will normally determine whether targets moving in close proximity will be detected as individual targets.

The proposed scheme is able to detect the correct number of targets if their velocities v_m are sufficiently apart in order to induce distinct peaks in (21). For this to occur, the velocity differences should be greater than the reciprocal of the digital spotlight region dimensions. Otherwise, if there are several targets with similar velocities and directions inside the same resolution cell, they will not be resolved and will be detected as a single target.

As a summary, the DMTI algorithm requires the following main steps:

a) One run of the wavefront reconstruction algorithm to image the target area with N_x (slant-range) by N_y (cross-range) samples;

b) For each region where moving targets may be present:

i) Digitally spotlight the region with size N_{sx} (slant-range) by N_{sy} (cross-range) and resynthesize its signature to the (ω, u) domain;

ii) Obtain reference signal $s_m(\omega, u)$ from the resynthesized signature, for a fixed ω;

iii) For a range of velocities v and angles θ of interest compute (16), (17), (18) and (21).

3.3.1 Potential Scenarios of Application

It can be applied for ground moving target indication in scenes where the relative velocity of the targets with respect to the radar platform is not sufficient to make them exoclutter targets.

Good for situations scenarios with dense road networks since the DTMI is able to filter out the vehicles that are not moving in the roads under study.

3.3.2 Advantages/Drawbacks

+ Useful for scenes with SCR greater than 10 dB in the spotlighted region.

+ Accuracy is approximately equal to that of the previous SAR ambiguity function but for scenarios with 2 dB lower SCR.

+ Ability to detect endoclutter targets provided that there is a previous digital spotlight of the region under analysis.

+ Ability to solve the blind angle ambiguity.

+ Reduces the overall computational requirements of the overall system since, due to the filtering of undesired targets, there will be a smaller number of targets to process and to perform consistency checks.

- Requires a priori information about the road network to perform traffic extraction and analysis.

- Velocity differences between the several targets to detect, inside the same spotlighted region, shall be greater than the reciprocal of the digital spotlight region dimensions.

3.4 Moving Targets with Velocities Beyond the Limit Imposed by the PRF

A moving target induces in the synthetic aperture radar returned signal a Doppler-shift and a Doppler-spread in the slow-time domain and fast-time domain, respectively. Given a pulse repetition frequency (PRF), the Doppler-shift is $f_D = 2v_x/\lambda$, where v_x is the target slant-range velocity and λ is the signal wavelength, is confined to

$$-\frac{PRF}{2} < f_D \leq \frac{PRF}{2}. \tag{22}$$

If the received signal is aliased (i.e., the induced Doppler-shift exceeds $PRF/2$ it has been mostly accepted that the true moving target slant-range velocity cannot be uniquely determined using a single antenna and a single pulse scheduling. Classical solutions to process such targets with a single channel consist in increasing the PRF or, alternatively, in using a non-uniform PRF [10]. However, increasing the PRF shortens the unambiguous range swath and increases the memory requirements to store the received signal. The use of a non-uniform PRF also has de drawback of requiring a non-conventional pulse scheduling, introducing complexity in the hardware and in the signal processing algorithms.

In [10] a new methodology is presented to retrieve slant-range velocity estimates of moving targets inducing Doppler-shifts beyond the Nyquist limit determined by the PRF. The proposed approach exploits the linear dependency (not subject to PRF limitations) of the Doppler-shift with respect to the slant-range velocity, at each wavelength. Basically, the algorithm computes the skew of the two-dimensional spectral signature of a moving target. Distinctive features of this algorithm are its ability to cope with strong range migration and its efficiency from the computational point of view.

By combining the developed scheme to retrieve the slant-range velocity with the SAR ambiguity function presented in the previous section, which estimates α, the full velocity vector is unambiguously retrieved without increasing the PRF.

Let $p(t)$ be the transmitted pulse when the antenna is at cross-range coordinate u and $S_m(u,t)$ the corresponding received signal. The 2D Fourier transform of the received signal, $S_m(k_u,k)$, where $k_u = 2\pi/\lambda_u$ is the slow-time frequency domain and $k \equiv 2\pi/\lambda$ is the fast-time frequency domain is, after pulse compression, given by [1]:

$$S_m(k_u,k) = |P(\omega)|^2 A(k_u,k) f_m e^{-j\sqrt{4k^2-\left(\frac{k_u}{\alpha}\right)^2}X} e^{-j\frac{k_u}{\alpha}Y}, \tag{23}$$

where $P(\omega)$ is the Fourier transform of the transmitted pulse $p(t)$ and $\omega = 2\pi/\lambda$. Symbols λ and λ_u denote the signal wavelength in the fast-time and in the slow-time frequency domain, respectively, and c is the speed of light. Function $A(k_u,k)$ is the two-way antenna radiation pattern. Symbol $\alpha \equiv \sqrt{\mu^2+\nu^2}$ is the relative speed of the moving target with respect to the radar, where $\nu \equiv (1+\frac{v_y}{V})$ and $\mu \equiv v_x/V$ denote, respectively, the moving target relative cross-range and slant-range velocities, with respect to the sensor velocity. The couple (X,Y) refers to the motion transformed coordinates of the moving target and are a rotated and scaled version of coordinates (x_0,y_0).

Relatively to a static target, and for a constant wavenumber k, the shape g becomes dilated by 2ν and shifted by $2k\mu$. If the transmitted pulse has bandwidth B, then k is confined to:

$$k_{min} \cong -\frac{\pi B}{c} + k_0 < k \leq k_0 + \frac{\pi B}{c} \cong k_{max}, \tag{24}$$

where $k_0 \equiv 2\pi/\lambda_0$ and λ_0 is the carrier wavelength. For a moving target with relative slant-range velocity μ, that the support of the returned signal $S_m(k_u,k)$ will exhibit a slope of 2μ with respect to the k axis, as illustrated in Figure 6. In this figure $k_{u_{end}}$, and $k_{u_{start}}$ denote the Doppler-shifts at the fast-time frequencies, respectively.

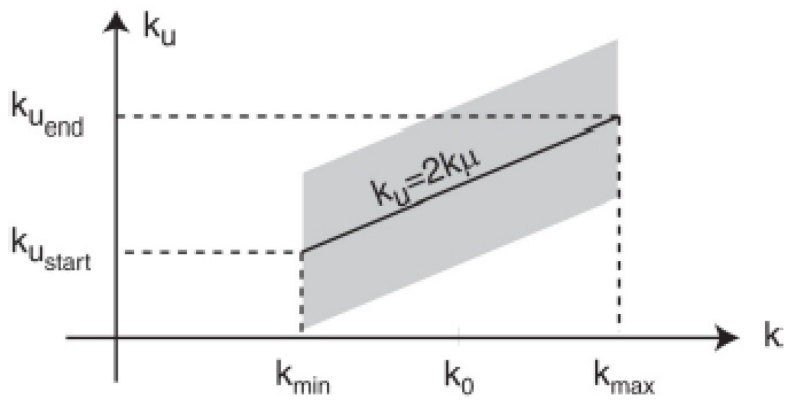

Figure 6: Support of the Returned Signal from a Moving Target with Relative Range Velocity μ.

We conclude then that:

$$\mu = \frac{k_{u_{end}} - k_{u_{start}}}{2(k_{max} - k_{min})}, \tag{25}$$

regardless of the PRF.

In the absence of electronic noise and ground clutter, $k_{u_{end}}$ and $k_{u_{start}}$ could be inferred using a simple centroid technique. This solution cannot, however, be applied when dealing with ground moving targets, because the returned signal co-exists with clutter returns in the 2D spectrum. The weight of the clutter can be reduced by digitally spotlighting the moving target area as shown previously. Once the moving target signature is spotlighted in the spatial domain, it is resynthesized back to the 2D frequency domain for further processing.

To deal with the clutter presence, and in order to estimate the spectrum skew, the authors propose to compute the autocorrelation function $R_{SS}(\Delta k_u, k_1, k_2)$ between $S_m(k_u, k_1)$ and $S_m(k_u, k_2)$ with respect to k_u, i.e.

$$\begin{aligned} R_{SS}(\Delta k_u, k_1, k_1 + \Delta k) \quad \approx \quad & |P(\omega_1)|^2 |P(\omega_2)|^2 |f_m|^2 e^{-j\left[\frac{\Delta k_u}{\alpha} Y - \left(2\Delta k - \frac{\Delta k_u^2}{4(k_1+\Delta k)\alpha^2}\right) X\right]} \\ & \times \int_{-\infty}^{+\infty} A(k_u, k_1) A^*(k_u - 2\Delta k\mu - \Delta k_u, k_1) e^{-j\phi} dk_u \,, \end{aligned} \tag{26}$$

where $\omega_1 = k_1 c$, $\omega_2 = k_2 c$, $\Delta k = k_2 - k_1$, and:

$$\phi = \frac{2k_u \Delta k_u}{4(k_1 + \Delta k)\alpha^2} X \tag{27}$$

If phase ϕ has an excursion smaller than π in the Doppler interval equivalent to the antenna *bandwidth* (herein we use the term antenna bandwidth to designate the slow-time wavenumber interval corresponding to the -3 dB two-way beamwidth of the antenna), the last line of (26) is a correlation between $A(k_u, k_1)$ and $A(k_u - 2\Delta k\mu, k_1)$, with respect to k_u, computed at Δk_u. The correlation magnitude $|R_{SS}(\Delta k_u, k_1, k_1 + \Delta k)|$ exhibits a maximum that is linearly dependent on Δk by a factor of 2μ.

The maximum relative slant-range velocity that can be estimated using this methodology is thus imposed by the above referred restriction on phase ϕ. To compute an expression for the maximum relative slant-range velocity that can be estimated, let us consider that the maximum magnitude of the correlation R_{SS} occurs at $\Delta k_u = 2\Delta k\mu$ and that the two-way antenna bandwidth is B_u [rad/m].

Considering that the relative velocity is $\alpha \approx 1$, then the relative slant-range velocity that can be estimated is bounded by:

$$|\mu| < \frac{(k + \Delta k)\pi}{B_u \Delta k X}. \tag{28}$$

Bound (28) can be made larger by compensating in (23) the dependency on X using the target area approximate slant-range coordinates; i.e., multiplying signal $S_m(k_u, k)$ by:

$$e^{j\sqrt{4k^2 - (k_u/\alpha')^2} X'} \tag{29}$$

where $X'$is the target approximate slant-range coordinate in the unfocused image and $\alpha' = 1$ is the target approximate velocity vector magnitude. In this way, phase ϕ, although not completely compensated, will exhibit a smaller excursion.

The method gives effective results even when the returned echoes of the moving targets and the static ground overlap completely, provided that the moving targets signatures are digitally spotlighted and the signal-to-clutter ratio is, roughly, greater than 14dB. The effectiveness of the method is illustrated with simulated and real data. As an example, slant-range velocities of moving objects with velocities between 6 and 12 times the Nyquist velocity are estimated with accuracy better than 3%.

3.4.1 Potential Scenarios of Application

Applied on GMTI for scenarios with fast moving targets that would, otherwise, require higher PRF.

3.4.2 Advantages/Drawbacks

+ Supports targets with velocities above the Nyquist limit imposed by the PRF.

- Only estimates the range velocity although it can be combined with other techniques, such as the previously described SAR ambiguity function, to estimate the complete velocity vector.

- Requires digital spotlight of the scene.

3.5 Ship Detection Using CFAR

Adaptive threshold algorithms are commonly used for target detection in SAR imagery [11], [12]. Their working principle is very simple: search for pixel values that are unusually bright compared with the ones in the surrounding area. The implementation of such algorithm is done by setting a threshold that is dependent of the surrounding area.

The constant false alarm rate (CFAR) detector is very popular and uses a window with 3 areas: test area, guard area and background area.

The SAR system resolution and the ship size need to be taken into consideration to define the detector window sizes. Typically the target window should be of similar size of the smallest ship to detect and the guard window should be of the size of the largest ship.

The background window has to be larger than the guard window to accommodate the background statistics. However it should not be so large that it no longer analyses the image locally.

The techniques based on CFAR detection use typically the histogram of the background window and select the threshold to the appropriate value in the tail of the distribution.

The background is modelled as having a certain parametric probability density function $f_c(x)$. The parameters of the selected density function are estimated from the background samples and the probability of false alarm p_{fa} for the threshold η_T is calculated using:

$$P_{fa} = 1 - \int_{-\infty}^{\eta T} f_c(x)dx = \int_{\eta T}^{\infty} f_c(x)dx. \tag{30}$$

The analytic calculation of the threshold η_T is not always possible, being used numerical methods to solve the problem. In some systems the value of η_T is chosen by trial and error. Many times, $f_c(x)$ is modelled as a Gaussian distribution since it is a good approximation. In these situations, the detector declares the presence of a target if:

$$x_t > \mu_b + \sigma_b t \tag{31}$$

where x_t is the value of the pixel under test, μ_b is the background mean and σ_b is the background standard deviation. Parameter t controls the false alarm rate and varies typically between 5, for low resolution images (i.e. single pixel targets) , and 6.5 for higher resolution images where the targets occupy several pixels (empirical parameters for ship detection in TerraSAR-X images [12]).

3.5.1 Potential Scenarios of Application

Ship detection in scenarios with SCR>=10 dB.

3.5.2 Advantages/Drawbacks

+ High detection accuracy.

+ Good results if discrimination algorithms are also used.

- Threshold is, typically, established by trial and error.

- Sensitive to strong metrological conditions (i.e. sea states).

3.6 Ship Velocity Estimation Using Single Look Complex Data

Ship velocity estimation using a sequence of single look SAR images has many similarities with the technique explained in the previous chapter [12]. The first step consists, as previously explained, on the generation of a sequence of single-look SAR images followed by detection of moving objects. The last operation consists in compensating the ship motion, once its motion parameters have been estimated, and imaging it.

The detection of ship candidates and its velocity estimation is based on a sequence of single-look images, where the moving targets change their positions from image to image. The estimation of the ship velocity follows a procedure which is similar to that previously explained in the GMTI section. The velocity of the ship is estimated by doing azimuth-split decomposition using bandpass filters. For a sequence of two images, the ship velocity in azimuth is approximately given by:

$$v_a \approx -\frac{\Delta x \cdot dx \cdot V}{\Delta f \cdot \lambda \cdot R_0}, \tag{32}$$

where Δx is the displacement vector, dx is the pixel resolution and Δf is the distance between the center frequency of the two sublooks. The accuracy of the velocity estimation depends on the accuracy of the displacement vector estimation Δx. The quantity Δx can be estimated with reasonable accuracy by measuring the distance between the centers of mass of the azimuth distributions of the target in the two sublooks.

The displacement vector is calculated accordingly to:

$$\Delta x = |c_1 - c_2| \tag{33}$$

where c_1 and $c_2$are the centers of mass of sublooks 1 and 2. The center of mass is computed by:

$$c_i = \frac{\sum_j m_{ij} x_{ij}}{\sum_j m_{ij}}, \tag{34}$$

where the sum is over the number of pixels belonging to the target in the *i*th look, m_{ij} represents the amplitude value and x_{ij} is the position of the *i*th look at time position *j*. The range velocity component is computed using the temporal shift between the two images, as follows:

$$v_r = \frac{\Delta t \cdot V}{R_0 \sin \theta'} \tag{35}$$

where Δt is the temporal shift and θ is the local incidence angle.

The estimation of the temporal shift Δt is computed by weighting the signal amplitude in each image with the time t_i of the image. Note that especially for spaceborne systems shift between the sublooks is not very sensitive to the range velocity component.

Originally this sublook technique was foreseen for data where no range cell migration has been performed.

3.6.1 Potential Scenarios of Application

Ship detection and velocity estimation in low SCR scenes.

3.6.2 Advantages/Drawbacks

+ Gives good results for SCR≥0 dB.

+ Estimates both velocity components.

- Azimuth accuracy depends on the precision of ship image center of mass estimation.

- Sublooks not very sensitive to range velocity component.

4.0 CONCLUSION

This paper summarized some state of the art algorithms for processing moving targets using single channel SAR data. It was shown that in order to obtain focused and correctly positioned moving objects in the SAR image the reconstruction algorithm must include information about the targets motion.

The blind angle ambiguity, which consists on the impossibility of obtaining the full velocity vector of moving objects using single channel SAR, can be solved if information about the antenna pattern is included.

To deal with endoclutter targets, the digital spotlight technique was presented, which is able to synthetically increase the SCR. A SAR ambiguity function for ground moving target indication, supported on the results obtained with the digital spotlight technique, was presented. Although it is able to detect the moving objects and to estimate the velocity vector magnitude, it cannot estimate the direction of motion.

To deal with the blind angle ambiguity, the Directional Moving Target Indication technique was presented. It is able to discriminate targets in a predefined direction of interest while simultaneously reducing the contribution of targets that move in other directions. The application of this methodology is mainly traffic monitoring.

A technique to deal with targets having velocities beyond the limit imposed by the pulse repetition frequency was also described. The algorithm uses the 2D spectrum skew to solve the limitation, having accuracy proportional to the emitted pulse bandwidth.

For ship detection and velocity estimation, techniques CFAR and a sequence of single look complex data were also presented.

5.0 ACKNOWLEDGEMENTS

The author wishes to acknowledge Prof. José-Bioucas Dias for the joint research activity carried together along several years that resulted in some of the publications and techniques that are herein summarized.

6.0 REFERENCES

[1] J. Dias and P. Marques, "Multiple moving targets detection and trajectory parameters estimation using a single SAR sensor," IEEE Transactions on Aerospace and Electronic Systems, Vol. 39, pp. 604-624, April 2003.

[2] J. Ender, P. Berens, A. Brenner, L. Rossing, U. Skupin, "Multi-channel SAR/MTI system development at FGAN: from AER to PAMIR", Proc. of IEEE Int. Geoscience Remote Sensing Symposium, IGARSS, 24-28 June 2002.

[3] S. Ochs, W. Pitz, "The TerraSAR-X and TanDEM-X Satellites", Recent Advances in Space Technologies, 3rd International Conference on, RAST, pp. 294-298, 14-16 June 2007.

[4] J. Curlander, R. McDonough, "Synthetic Aperture Radar, Systems and Signal Processing", Wiley 1991.

[5] S. Hinz, F. Meyer, A. Laika, R. Bamler, "Spaceborne traffic monitoring with Dual Channel Synthetic Aperture Radar – Theory and Experiments", Proc. of IEEE, Computer Society Conference on, Vol. 3, pp. 7-7, 20-26 June 2005.

[6] J. Ender, "Space-Time Adaptive Processing for Synthetic Aperture Radar", IEE Colloquium on Space-Time Adaptive Processing (Ref. No. 1998/241), pp. 611-618, April 1998.

[7] M. Soumekh, Synthetic Aperture Radar Signal Processing with MATLAB algorithms. WILEY-INTERSCIENCE, 1999.

[8] M. Soumekh, "Reconnaissance with ultra wideband UHF synthetic aperture radar", IEEE Signal Processing Magazine, pp. 21-40, 1995.

[9] P. Marques, "Directional moving target indication: A novel SAR ambiguity function for traffic monitoring," Hindawii Journal of Electrical and Computer Engineering, Vol. 2012, March 2012.

[10] P. Marques and J. Dias, "Velocity estimation of fast moving targets using a single SAR sensor", Aerospace and Electronic Systems, IEEE Transactions on, Vol. 41, No. 1, pp. 75-89, January 2005.

[11] D. J. Crisp, The state-of-the-art in ship detection in SAR. Intelligence Surveillance and Reconnaissance Division, 2004.

[12] S. Brusch, S. Lehner, T. Fritz, M. Soccorsi, A. Soloviev, and B. van Schie, "Ship surveillance with terrasar-x," Geoscience and Remote Sensing, IEEE Transactions on, Vol. 49, No. 3, pp. 1092-1103, March 2011.

[13] V. Chen, "Detection of ground moving targets in clutter with rotational wigner-radon transforms," in Proceedings of the EUSAR'02, 2002, pp. 229-232.

[14] C. Rossi, H. Runge, H. Breit, and T. Fritz, “Surface current retrieval from terrasar-x data using Doppler measurements,” in Geoscience and Remote Sensing Symposium (IGARSS), 2010 IEEE International, July 2010, pp. 3055-3058.